# Accelerometers on Quadrotors: What do they Really Measure?

P Martin

**P. Martin**
(Mines ParisTech)

E-mail : philippe.martin@mines-paristech.fr

DOI : 10.12762/2014.AL08-06

# Accelerometers on Quadrotors : What do they Really Measure?

A revisited quadrotor model is proposed, including the so-called rotor drag. It differs from the model usually considered, even at first order, and much better explains the role of accelerometer feedback in control algorithms. The theoretical derivation is supported by experimental data.

## Introduction

Quadrotor control has been an active area of investigation for several years. On the one hand, the quadrotor has several qualities, among them its very simple mechanical design, and qualifies as a viable concept of mini Unmanned Aerial Vehicle (UAV) for real-life missions ; on the other hand, it is perceived in the control community as a very rich case study in theoretical and applied control. The first control objective is to ensure a stable flight at moderate velocities and, in particular, in hovering; this fundamental building block is then used to develop higher-level tasks.

However, for experiments designed to work only in the lab with an off-board measuring device, e.g. [1], quadrotors all rely at the heart on strapdown MEMS inertial sensors (gyroscopes and accelerometers). These inertial sensors may be used alone (as far as horizontal stabilization is concerned) [2], or supplemented by other sensors, which usually provide some position-related information. Representative designs are: ultrasonic rangers [3]; (simple) GPS module when outdoors and infrared rangers when indoors [4] ; carrier phase differential GPS [5]; laser rangefinder [6]; vision system [7], [8], [9] ; laser rangefinder and vision system [10], [11]. Unfortunately those extra sensors have inherent drawbacks (low bandwidth, possible temporary unavailability, etc.), hence inertial sensors remain essential for basic stabilization.

Nearly all of the papers in the literature rely on the same physical model: only aerodynamic forces and moments proportional to the square of the propeller angular velocities are explicitly taken into account. Other aerodynamic effects are omitted and considered as small non-modeled disturbances to be rejected by the control law. The reason put forward is that these effects are proportional to the square of the quadrotor linear velocity, hence very small near hovering. Few authors explicitly consider other aerodynamic effects : [12] notes the importance of flapping stability derivatives; [13] and [14] consider aerodynamic effects without physical motivation linear with respect to the quadrotor linear and angular velocities, but propose very small numerical values; [5] judges them to be negligible at low velocities, and focuses on nonlinear aspects at moderate velocities; [15] physically motivates the presence of effects that are nearly linear with respect to the quadrotor linear and angular velocities, but provides no experimental data and is concerned only with the open-loop system.

Figure 1 - Our home-built quadrotor : the “Quadricopter”

On the other hand, the accelerometer measurement vector $\vec{a}$ can be used in two different ways (gyros are used in both cases ; see page 4 for more details about inertial sensors):

1) as an input, directly in the equation $\dot{\vec{V}} = \vec{g} + \vec{a}$ if extra sensors providing position or velocity information are available, using a sensor fusion algorithm that estimates the velocity and the pitch and roll angles

2) as an output, through the approximation $\vec{a} \approx -\vec{g}$ . Accordingly, the pitch and roll angles are estimated by a sensor fusion algorithm. Commercial "attitude sensors", such as the 3DM-GX[1] or the MTi[2], run exactly on this principle.

In both cases, the sensor fusion algorithm can be an Extended Kalman Filter (EKF), a complementary filter, linear or nonlinear, or a nonlinear observer; see for example [16], [17] for an account of the two cases. Recall that MEMS inertial sensors are not accurate enough for "true" Schuler-based inertial navigation, see for example [18, Chap. 5] for details.

Now, a puzzling issue arises: the "conventional" physical model implies that the longitudinal and lateral (in body axes) accelerometers should always measure zero, which clearly contradicts 2) ; as for 1), even if no particular form of the accelerometers measurements is assumed, one may wonder about the interest of using measurements known to be zero (in addition corrupted by noise and biases). Nevertheless, many successful quadrotor flights have been reported, with control laws based on 1) or 2), or even both, and there is no question that using accelerometers is beneficial.

This paper, which largely draws on [19], proposes a "revisited" model containing extra aerodynamic terms proportional to the propeller angular velocity times the quadrotor linear or angular velocity. In particular, the so-called rotor drag, though rather small, appears at first order and is essential to correctly account for the accelerometer measurements.

The paper is structured as follows: the revisited model is derived in next section ; its main features are experimentally validated then ; finally, its implications for control schemes are discussed.

## A revisited quadrotor model

### Model of a single propeller "near" hovering

We first consider a single propeller rotating with angular velocity $\varepsilon_i \omega_i$ around its axis $k_b$; $\omega_i$ is positive, with $\varepsilon_1 = 1$ (resp. -1) for counterclockwise (resp. clockwise) rotation. Due to the motion of the quadrotor, the geometric center $A_i$ of the propeller moves with linear velocity $\vec{V}_{A_i}$, while the rotor plane (by definition perpendicular to $\vec{k}_b$) undergoes angular velocity $\vec{\Omega}$; the total angular velocity of the propeller is thus $\vec{\Omega} + \varepsilon_1 \omega_i \vec{k}_b$. A lengthy derivation in the spirit of for example [20, in particular Chap. 5] shows that the aerodynamic efforts on the propeller resolve into the force $\vec{F}_i$ and moment $\vec{M}_i$ at $A_i$ ,

$$\vec{F}_i = -a\omega_i^2 \vec{k}_b - \omega_i \left( \lambda_1 \vec{V}_{A_i}^{\perp} + \lambda_2 \vec{\Omega} \times \vec{k}_b \right) - \varepsilon_i \omega_i \left( \lambda_3 \vec{V}_{A_i} \times \vec{k}_b + \lambda_4 \vec{\Omega}^{\perp} \right) \quad (1)$$

$$\vec{M}_i = -b\varepsilon_i \omega_i^2 \vec{k}_b - \varepsilon_i S \omega_i \left( \mu_1 \vec{V}_{A_i}^{\perp} + \mu_2 \vec{\Omega} \times \vec{k}_b \right) - \omega_1 \left( \mu_3 \vec{V}_{A_i} \times \vec{k}_b + \mu_4 \vec{\Omega}^{\perp} \right) \quad (2)$$

where $a, b,$ the $\lambda_i$'s and $\mu$'s are positive constants ; the projection of a vector $\vec{U}$ on the rotor plane is denoted by

$$\vec{U}^{\perp} = \vec{k}_b \times \left( \vec{U} \times \vec{k}_b \right) = \vec{U} - \left( \vec{U} \cdot \vec{k}_b \right) \vec{k}_b$$

Moreover $\lambda_2$ and $\mu_2$ are very small (they would be exactly zero if the blade axis were orthogonal to $\vec{k}_b$ ). Notice that all of the force and moment terms orthogonal to $\vec{k}_b$ arise from the velocity imbalance of the blade on a complete turn (because of the translational motion, the blade moves faster with respect to free air when it is advancing than when it is retreating).

The above relations rely on classical blade element theory, with two extra assumptions:

- the propeller is considered to be perfectly rigid, which is approximately true for most quadrotor propellers. The flapping due to the slight flexibility of a real propeller has only a marginal effect ;
- the components of the linear velocity $\vec{V}_{A_i}$ are considered small with respect to the propeller tip speed ; similarly the components of the angular velocity $\vec{\Omega}$ are considered to be small with respect to $\omega_i$ . This is valid "near" hovering, i.e., for "small" $\vec{V}_{A_i}$ and $\vec{\Omega}$ : typically, the tip speed is of about $50\, m.s^{-1}$ , so that $10\, m.s^{-1}$ can still be seen as a "small" velocity.

The velocities in the previous equations are of course velocities with respect to the air stream, not with respect to the ground. They coincide when there is no wind, which we assume in the sequel.

The term $\omega_i \lambda_1 \vec{V}_{A_i}^{\perp}$ in (1) is often called $H$-force or rotor drag in the helicopter literature. Also notice that the simplified expressions (1)-(2), though directly based on textbook helicopter aerodynamics, do not seem to appear in the literature under this compact form, very handy for control purposes. The reason for this is probably that helicopter literature is primarily concerned with articulated and/or rather flexible propellers, operating moreover at much higher ratios of linear velocity to propeller tip speed.

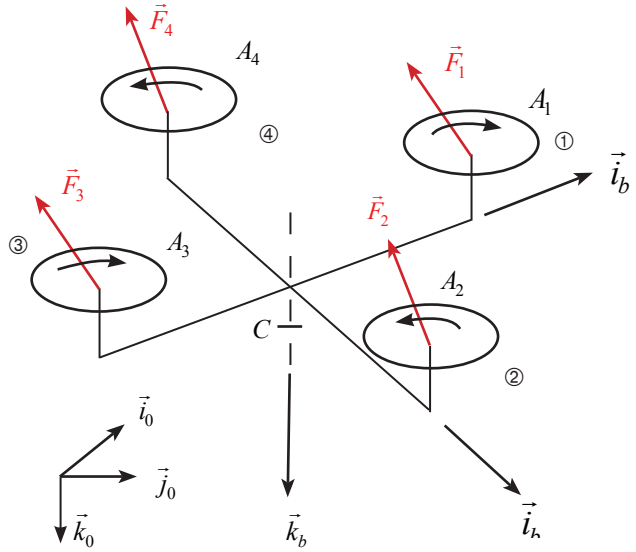


Figure 2 - Sketch of the complete quadrotor

### Complete quadrotor model

The quadrotor consists of a rigid frame with four propellers, (directly) driven by electric motors, see figure 2. The structure is symmetrically

[1] www.microstrain.com
[2] www.xsens.com

arranged, with one pair of facing propellers rotating clockwise and the other pair rotating counterclockwise. The four propellers have the same axis $\vec{k}_b$.

$\vec{i}_b = \frac{\overrightarrow{A_3A_1}}{\|\overrightarrow{A_3A_1}\|}$, $\vec{j}_b = \frac{\overrightarrow{A_4A_2}}{\|\overrightarrow{A_4A_2}\|}$ and $\vec{k}_b$ thus form a direct coordinate frame.
Let $A$ be the geometric center of the $A_1's$ and $l = \frac{1}{2}\|\overrightarrow{A_3A_1}\| = \frac{1}{2}\|\overrightarrow{A_2A_4}\|$;

clearly, $\sum_{i=1}^{4} \overrightarrow{AA_i} = 0$.

The whole system $\mathcal{B}$, with mass m and center of mass $C$, thus involves five rigid bodies : the frame/stator assembly $\mathcal{B}_0$ and the four propeller/motor assemblies $\mathcal{B}_i$. Clearly $\overrightarrow{CA} = h\vec{k}_b$ for some (signed) length $h$; notice that for most quadrotor designs $h$ is very small. Resolved in the $(\vec{i}_b, \vec{j}_b, \vec{k}_b)$ frame, the velocity of $C$ is written as $\vec{V}_C = u\vec{i}_b + v\vec{j}_b + w\vec{k}_b$ and the angular velocity of $\mathcal{B}_0$ is written as $\vec{\Omega} = p\vec{i}_b + q\vec{j}_b + r\vec{k}_b$

We assume that the only efforts acting on $\mathcal{B}$ are the weight and the aerodynamic efforts created by the propellers, as described in the previous section. In particular, we neglect the drag created by the frame, which is quadratic with respect to the velocity, hence small at low velocities with respect to the rotor drag. Newton's laws for the entire system are thus written as

$$m\,\dot{\vec{V}}_C = m\,\vec{g} + \sum_{i=1}^{4} \vec{F}_i \tag{3}$$

$$\dot{\vec{\sigma}}_C^{\mathcal{B}} = \sum_{i=1}^{4} \overrightarrow{CA_i} \times \vec{F}_i + \vec{M}_i \tag{4}$$

where $\vec{\sigma}_C^{\mathcal{B}} = \int_{\mathcal{B}} \overrightarrow{CM} \times \dot{\overrightarrow{CM}}\, d\mu(M)$ is the kinetic momentum of $\mathcal{B}$. For each $\mathcal{B}_i$, we can further write

$$\dot{\vec{\sigma}}_{A_i}^{\mathcal{B}_i} \cdot \vec{k}_b = \vec{M}_i \cdot \vec{k}_b + \varepsilon_i \Gamma_i \tag{5}$$

where $\vec{\sigma}_{A_i}^{\mathcal{B}_i} = \int_{\mathcal{B}_i} \overrightarrow{A_iM} \times \dot{\overrightarrow{A_iM}}\, d\mu(M)$ is the kinetic momentum of $\mathcal{B}_i$ and $\Gamma_i$ is the (positive) electromagnetic torque of the motor. For simplicity, we have considered $A_i$ as the center of mass of $\mathcal{B}_i$ (in fact the two points are slightly apart). We also consider the $\Gamma_i's$ as the control inputs (it is nevertheless easy to include the behavior of the electric motors, both for modeling and control).

We now evaluate the right-hand sides of (3)-(4). Since

$$\vec{V}_{A_i} = \vec{V}_C + \overrightarrow{CA} + \overrightarrow{AA_i} = \vec{V}_C + h\vec{\Omega} \times \vec{k}_b + \vec{\Omega} \times \overrightarrow{AA_i}$$

we have

$$\begin{aligned}
&\lambda_3 \vec{V}_{A_i} \times \vec{k}_b + \lambda_4 \vec{\Omega}^{\perp} \\
&\quad = \lambda_3 (\vec{V}_C + h\vec{\Omega} \times \vec{k}_b + \vec{\Omega} \times \overrightarrow{AA_i}) \times \vec{k}_b + \lambda_4 \vec{\Omega}^{\perp} \\
&\quad = \lambda_3 \vec{V}_C \times \vec{k}_b + \lambda'_4 \vec{\Omega}^{\perp} + r\lambda_3 \overrightarrow{AA_i}
\end{aligned}$$

$$\begin{aligned}
&\lambda_1 \vec{V}_{A_i}^{\perp} + \lambda_2 \vec{\Omega} \times \vec{k}_b \\
&\quad = \lambda_1 (\vec{V}_C^{\perp} + (h\vec{\Omega} \times \vec{k}_b)^{\perp} + (\vec{\Omega} \times \overrightarrow{AA_i})^{\perp} + \lambda_2 \vec{\Omega}^{\perp} \quad k_b \\
&\quad = \lambda_1 \vec{V}_C^{\perp} + \lambda'_2 \vec{\Omega} + \vec{k}_b - r\lambda_1 \overrightarrow{AA_i} \times \vec{k}_b
\end{aligned}$$

where we have used the fact that $\overrightarrow{AA_i}$ is collinear to either $\vec{i}_b$ or $\vec{j}_b$, and set $\lambda'_2 = \lambda_1 + h\lambda_1$ and $\lambda'_4 = \lambda_4 + h\lambda_3$. Therefore,

$$\begin{aligned}
\sum_{i=1}^{4} \vec{F}_i &= -a\left(\sum_{i=1}^{4} \omega_i^2\, \vec{k}_b\right) - \left(\sum_{i=1}^{4} \omega_i\right)(\lambda_1 \vec{V}_C^{\perp} + \lambda'_2\, \vec{\Omega} \times \vec{k}_b) \\
&\quad - \left(\sum_{i=1}^{4} \varepsilon_i \omega_i\right)(\lambda_3 \vec{V}_C \times \vec{k}_b + \lambda'_4\, \vec{\Omega}^{\perp}) \\
&\quad + r\lambda_1 \left(\sum_{i=1}^{4} \omega_i \overrightarrow{AA_i}\right) \times \vec{k}_b - r\lambda_3 \left(\sum_{i=1}^{4} \varepsilon_i \overrightarrow{AA_i}\right) \\
&\approx -a\left(\sum_{i=1}^{4} \omega_i^2\right) \vec{k}_b - \left(\sum_{i=1}^{4} \omega_i\right)(\lambda_1 \vec{V}_C^{\perp} + \lambda'_2\, \vec{\Omega} \times \vec{k}_b)
\end{aligned}$$

In the last line, we have neglected small terms according to the second extra assumption of the single properller model. Indeed, in hovering $\vec{V}_C$ and $\vec{\Omega}$, hence $\vec{V}_{A_i}$ are zero ; from (1)–(4) this implies that
$a(\omega_1^2 + \omega_2^2 + \omega_3^2 + \omega_4^2) = mg$
and $\omega_1^2 - \omega_2^2 + \omega_3^2 - \omega_4^2 = \omega_1^2 - \omega_3^2 = \omega_2^2 - \omega_4^2 = 0$,
and eventually $\omega_i = \bar{\omega} = \sqrt{\frac{mg}{4a}}$ .

As a consequence $\sum_{i=1}^{4} \varepsilon_i \omega_i$, $\frac{1}{l}\sum_{i=1}^{4} \omega_i \overrightarrow{AA_i}$ and $\frac{1}{l}\sum_{i=1}^{4} \varepsilon_i \omega_i, \overrightarrow{AA_i}$ also vanish in hovering ; "near" hovering they are therefore small with respect to $\sum_{i=1}^{4} \omega_i$ .

Similar computations yield

$$\begin{aligned}
&\sum_{i=1}^{4} \overrightarrow{CA_i} \times \vec{F}_i + \overrightarrow{AA_i} \times \vec{F}_i + \vec{M}_i \\
&\quad \approx -a\left(\sum_{i=1}^{4} \omega_i^2 \overrightarrow{AA_i}\right) \times \vec{k}_b - b\left(\sum_{i=1}^{4} \varepsilon_i \omega_i^2\right) \vec{k}_b \\
&\quad\quad - r\lambda_1 l^2 \left(\sum_{i=1}^{4} \omega_1\right) \vec{k}_b - \left(\sum_{i=1}^{4} \omega_1\right)(\mu'_3\, \vec{V}_C \times \vec{k}_b + \mu''_4\, \vec{\Omega}^{\perp})
\end{aligned}$$

where $\mu'_3 = \mu_3 - h\lambda_1$ and $\mu''_4 = \mu_4 + h(\mu_1 + \lambda'_2)$.

Notice that the contributions of $\lambda_3$, $\lambda_4$ in the forces (1) and of $\mu_1$, $\mu_2$ in the moments (2) (nearly) cancel out in the right-hand sides of (3)-(4), due to the fact there are two clockwise and two counterclockwise-rotating propellers.

We then evaluate the left-hand sides of (3)–(5). The approach is fairly standard.

$$\begin{aligned}
\vec{\sigma}_C^{\mathcal{B}} &= \int_{\mathcal{B}} \overrightarrow{CM} \times \dot{\overrightarrow{CM}}\, d\mu(M) \\
&= \int_{\mathcal{B}_0} \overrightarrow{CM} \times \dot{\overrightarrow{CM}}\, d\mu(M) \\
&\quad + \sum_{i=1}^{4} \int_{\mathcal{B}_1} \overrightarrow{CM} \times (\dot{\overrightarrow{CA_i}} + \dot{\overrightarrow{A_iM}})\, d\mu(M) \\
&= \int_{\mathcal{B}_0} \overrightarrow{CM} \times (\vec{\Omega} \times \overrightarrow{CM})\, d\mu(M) \\
&\quad + \sum_{i+1}^{4} \int_{\mathcal{B}_i} \overrightarrow{CM} \times (\vec{\Omega} \times \overrightarrow{CA_i} + (\vec{\Omega} + \varepsilon_i \omega_i \vec{k}_b) \times \overrightarrow{A_iM})\, d\mu(M) \\
&= \int_{\mathcal{B}} \overrightarrow{CM} \times (\vec{\Omega} \times \overrightarrow{CM})\, d\mu(M) \\
&\quad + \sum_{i=1}^{4} \int_{\mathcal{B}_1} \overrightarrow{A_iM} \times (\varepsilon_i \omega_i \vec{k}_b \times \overrightarrow{A_iM})\, d\mu(M) \\
&= \mathcal{I}_C^{\mathcal{B}} \cdot \vec{\Omega} + \sum_{i=1}^{4} \varepsilon_i \omega_i (\mathcal{I}_{A_i}^{\mathcal{B}_i} \cdot \vec{k}_b) \\
&= Ip\vec{i}_b + Iq\vec{j}_b + (Jr + J_r \sum_{i=1}^{4} \varepsilon_i \omega_i)\vec{k}_b
\end{aligned}$$

where $I; J; J_r$ are strictly positive constants. In the last equation, in the computation of the inertia tensors $\mathcal{I}^{\mathcal{B}}$, $\mathcal{I}_{A_i}^{\mathcal{B}_i}$ we have replaced

the actual propellers by disks with the same masses and radii, and taken advantage of the various symmetries ; this "averaging" approximation is justified by the fact that the propeller angles vary much faster than all of the other kinematic variables (besides, this approximation is already heavily used in the blade element theory used to derive (1)-(2)). Using the same approximation,

$$\begin{aligned}\vec{\sigma}_{A_i}^{\mathcal{B}_i} &= \int_{\mathcal{B}_i} \overrightarrow{A_iM} \times \overrightarrow{A_iM}\, d\mu(M) \\ &= \int_{\mathcal{B}_i} \overrightarrow{A_iM} \times (\vec{\Omega} + \varepsilon_i \omega_i \vec{k}_b) \times \overrightarrow{A_iM})\, d\mu(M) \\ &= \mathcal{I}_{A_i}^{\mathcal{B}_i} . (\vec{\Omega} + \varepsilon_i \omega_i \vec{k}_b) \\ &= I_r p \vec{i}_b + I_r q \vec{j}_b + J_r (r + \varepsilon_i \omega_i) \vec{k}_b\end{aligned}$$

where $I_r$ is a strictly positive constant. Eventually,

$$\begin{pmatrix} \dot{\vec{V}}_C \cdot \vec{i}_b \\ \dot{\vec{V}}_C \cdot \vec{j}_b \\ \dot{\vec{V}}_C \cdot k_b \end{pmatrix} = \begin{pmatrix} \dot{u} + qw - ru \\ \dot{v} + ru - pw \\ \dot{w} + pu - qu \end{pmatrix}$$

$$\begin{pmatrix} \dot{\vec{\sigma}}_C^{\mathcal{B}} . \vec{i}_b \\ \dot{\vec{\sigma}}_C^{\mathcal{B}} . \vec{j}_b \\ \dot{\vec{\sigma}}_C^{\mathcal{B}} . \vec{k}_b \end{pmatrix} = \begin{pmatrix} I\dot{p} + (J - I) qr + J_r q \sum_{i=1}^4 \varepsilon_i \omega_i \\ I\dot{q} + (J - I) pr + J_r p \sum_{i=1}^4 \varepsilon_i \omega_i \\ J\dot{r} + J_r \sum_{i=1}^4 \varepsilon_i \dot{\omega}_i \end{pmatrix}$$

$$\dot{\vec{\sigma}}_{C_i}^{\mathcal{B}_i} . \vec{k}_b = J_r (\dot{r} + \varepsilon_i \dot{\omega}_i) \qquad i = 1,2,3,4$$

To describe the orientation of the quadrotor, we use the classical $\phi, \theta, \Psi$ Euler angles (quaternions could of course be used). The direction cosine matrix $R_{\phi,\theta,\Psi}$ to convert from Earth coordinates to aircraft coordinates is then

$$\begin{pmatrix} C\theta C\psi & C\theta S\psi & -S\theta \\ S\phi S\theta C\psi - C\phi S\psi & S\phi S\theta S\psi + C\phi C\psi & S\phi C\theta \\ C\phi S\theta C\psi + S\phi S\psi & C\phi S\theta S\psi - S\phi S\psi & C\phi C\theta \end{pmatrix}$$

so that $g = g(-i \sin\theta + j \sin\phi\cos\theta + k \cos\phi\cos\theta)$.

Collecting the previous findings (3)–(5), we eventually have

$$\dot{u} + qw - rv = -g \sin\theta - u \frac{\lambda_1}{m} \sum_{i=1}^4 \omega_i \tag{6}$$

$$\dot{v} + ru - pw = g \sin\phi \cos\theta - v \frac{\lambda_1}{m} \sum_{i=1}^4 \omega_i \tag{7}$$

$$\dot{w} + pv - qu = g - \cos\phi\cos\theta - \frac{a}{m} \sum_{i=1}^4 \omega_i^2 \tag{8}$$

$$\begin{aligned} I\dot{p} + (J - I) qr + J_r q \sum_{i=1}^4 \varepsilon_i \omega_i \\ = a(\omega_1^2 - \omega_3^2) + (\mu_3' v + \mu_4'' p) \sum_{i=1}^4 \omega_i \end{aligned} \tag{9}$$

$$\begin{aligned} I\dot{q} - (J - I) pr - J_r p \sum_{i=1}^4 \varepsilon_i \omega_i \\ = a(\omega_1^2 - \omega_3^2) + (\mu_3' u - \mu_4'' q) \sum_{i=1}^4 \omega_i \end{aligned} \tag{10}$$

$$(J - 4J_r)\dot{r} = -\lambda_1 l^2 \sum_{i=1}^4 \omega_i - \sum_{i=1}^4 \varepsilon_i \Gamma_i \tag{11}$$

$$J_r (\varepsilon_i \dot{r} + \omega_i) = \Gamma_i - b\omega_i^2 \qquad i = 1,2,3,4 \tag{12}$$

In (6)–(7) we have assumed $\lambda'_2 = \lambda_2 + h\lambda_1 \approx 0$, which is sensible since $\lambda_2$ and $h$ are nearly 0 (notice that $\lambda'_2 = 0$ can always be enforced by slightly shifting the center of mass). Finally, the angles and angular velocities are linked by

$$\dot{\phi} = p + (q \sin\phi + r \cos\phi) \tan\phi \tag{13}$$

$$\dot{\theta} = q \cos\phi - r \sin\phi \tag{14}$$

$$\dot{\psi} = \frac{q \sin\phi + r \cos\phi}{\cos\theta} \tag{15}$$

Equations (6)–(15) form the complete 13-dimensional nonlinear model of the quadrotor.

A further simplification is to replace $\sum_{i=1}^4 \omega_i$ by $4\bar{\omega}$ in (6) – (12) since $\omega_i$ remains close to $\bar{w}$ in normal flight and moreover use the fact that the propeller moment of inertia $J_r$ is very small with respect to $J - I$ ; this yields

$$\dot{u} + qw - rv = -g \sin\theta - \frac{4\omega\lambda_1}{m} u \tag{16}$$

$$\dot{v} + ru - pw = -g \sin\phi\cos\theta - \frac{4\bar{\omega}\lambda_1}{m} v \tag{17}$$

$$\dot{w} + pv - qu = g \cos\phi\cos\theta - \frac{a}{m} \sum_{i=1}^4 \omega_i^2 \tag{18}$$

$$I\dot{p} + (J - I) qr = a(\omega_4^2 - \omega_2^2) 4\bar{\omega}(\mu'_3 v + \mu''_4 p) \tag{19}$$

$$I\dot{q} + (J - I) qr = a(\omega_4^2 - \omega_2^2) 4\bar{\omega}(\mu'_3 u + \mu''_4 p) \tag{20}$$

$$J\dot{r} = -4\bar{\omega}\lambda_1 l^2 r - \sum_{i=1}^4 \varepsilon_i \Gamma_i \tag{21}$$

$$J_r \dot{\omega}_i - \varepsilon_i \frac{4\bar{\omega}\lambda_1 l^2 J r}{I} r = \Gamma_i - b\omega_1^2, \quad i = 1,2,3,4 \tag{22}$$

Equations (16)–(22) can be used instead of (6)–(12) with no noticeable loss of accuracy.

## Model of the inertial sensors

The quadrotor is equipped with strapdown triaxial gyroscope and accelerometer. Without restriction, we assume that the sensing axes coincide with $\vec{i}_b, \vec{j}_b, \vec{k}_b$. The gyroscope measures the angular velocity $\vec{\Omega}$, projected on its sensing axes, i.e., $(g_x, g_y, g_z) = (p, q, r)$, the accelerometer measures the specific acceleration $\vec{a} = \dot{\vec{V}}_P - \vec{g}$ of the point $P$ where it is located, projected on its sensing axes; see for example [18, Chap. 4] for details on inertial sensors. Hence, by (3) if the accelerometer is located at the center of mass $C$, which is the case for most quadrotors, it measures

$$\vec{a} = \dot{\vec{V}}_C - \vec{g} = \frac{1}{m} \sum_{i=1}^4 \vec{F}_i$$

by (3), the accelerometer thus measures

$$a_x = \vec{a} . \vec{i}_b = -\frac{\lambda_1}{m} (\omega_1 + \omega_2 + \omega_3 + \omega_4) u \tag{23}$$

$$a_y = \vec{a} . \vec{j}_b = -\frac{\lambda_1}{m} (\omega_1 + \omega_2 + \omega_3 + \omega_4) v \tag{24}$$

$$a_z = \vec{a} . \vec{k}_b = -\frac{a}{m} (\omega_1^2 + \omega_2^2 + \omega_3^2 + \omega_4^2) \tag{25}$$

As in the previous section we can replace (23)–(24), without a noticeable loss of accuracy, by

$$a_x = -\frac{4\bar{\omega}\lambda_1}{m}u \tag{26}$$

$$a_y = -\frac{4\bar{\omega}\lambda_1}{m}v \tag{27}$$

This shows that $a_x$, $a_y$ actually measure the quadrotor longitudinal and lateral velocities (while $a_z$ measures the total thrust).

### Linearized model

To highlight the salient features of the revisited model (6)–(15) and its measurements, it is enough to consider its first order approximation. Suitably putting together variables, this linearized model can be divided into four independent subsystems :

- longitudinal subsystem (states $u,\ \theta,\ q, \omega_1 - \omega_3$ ; input $\Gamma_1 - \Gamma_3$ measurements $a_x \approx -\frac{4\bar{\omega}\lambda_1}{m}u$ and $g_y \approx q$ )

$$\dot{u} \approx -g\theta - \frac{4\bar{\omega}\lambda_1}{m}u$$
$$\dot{\theta} \approx q$$
$$I\dot{q} \approx 4\bar{\omega}\mu'_3\, u - 4\bar{\omega}\mu''_4\, q + 2al\bar{\omega}(\omega_1 - \omega_3)$$
$$J_r(\dot{\omega}_1 - \dot{\omega}_3) \approx \Gamma_1 - \Gamma_3 - 2b\bar{\omega}(\omega_1 - \omega_3)$$

- lateral subsystem (states $v,\ \phi,\ p,\ \omega_4 - \omega_2$ ; input $\Gamma_4 - \Gamma_2$ measurements $a_y \approx -\frac{4\bar{\omega}\lambda_1}{m}\ v$ and $g_x \approx p$ )

$$\dot{v} \approx -g\phi - \frac{4\bar{\omega}\lambda_1}{m}v$$
$$\dot{\phi} \approx p$$
$$I\dot{p} \approx -4\bar{\omega}\mu'_1\,\bar{\omega}v - 4\mu''_4\,\bar{\omega}p + 2al\bar{\omega}(\omega_4 - \omega_2)$$
$$J_r(\dot{\omega}_4 - \dot{\omega}_2) \approx \Gamma_4 - \Gamma_2 - 2b\bar{\omega}(\omega_4 - \omega_2)$$

- vertical subsystem (states $w, \sum_{i=1}^4 \omega_i$ input $\sum_{i=1}^4 \Gamma_i$ measurement $a_z \approx -g - \frac{2a\bar{\omega}}{m}\sum_{i=1}^4 \omega_i)$

$$\dot{w} \approx \frac{2a\bar{\omega}}{m}\left(4\bar{\omega} - \sum_{i=1}^4 \omega_i\right)$$
$$J_r \sum_{i=1}^4 \dot{\omega}_i \approx \sum_{i=1}^4 \Gamma_i - 2b\bar{\omega}\sum_{i=1}^4 \Gamma_i$$

- heading subsystem (states $\psi;\ r; \sum_{i=1}^4 \varepsilon_i\omega_i$; input $\sum_{i=1}^4 \varepsilon_i\Gamma_i$ measurement $g_z \approx r$ )

$$\dot{\psi} \approx r$$
$$J\dot{r} \approx -4\bar{\omega}\lambda_1 l^2 r - \sum_{i=1}^4 \varepsilon_i\Gamma_i$$
$$J_r \sum_{i=1}^4 \varepsilon_i\dot{\omega}_i \approx \frac{16\bar{\omega}\lambda_1 l^2 J_r}{J}r + \sum_{i=1}^4 \varepsilon_i\Gamma_i - 2b\bar{\omega}\sum_{i=1}^4 \varepsilon_i w_i$$

In the sequel we concentrate on the longitudinal system, where accelerometer feedback is of paramount importance (the lateral subsystem is the same up to a sign-reversing coordinate change). Setting $\omega_q = \omega_1 - \omega_3$, $\Gamma_q = \frac{\Gamma_1 - \Gamma_3}{J_r}$ and

$$(f_1, f_2, f_3, f_4, f_5) = \left(\frac{4\bar{\omega}\lambda_1}{m}, \frac{4\bar{\omega}\mu'_3}{I}, \frac{4\bar{\omega}\mu''_4}{I}, \frac{2al\bar{\omega}}{I}, \frac{2b\bar{\omega}}{J_r}\right)$$

the longitudinal subsystem is thus written as

$$\dot{u} = -f_1 u - g\theta \tag{28}$$
$$\dot{\theta} = q \tag{29}$$
$$\dot{q} = f_2 u - f_3 q + f_4\omega_q \tag{30}$$
$$\dot{\omega}_q = \Gamma_q - f_5\omega_q \tag{31}$$

with measurements $a_x = -f_1 u$ and $g_y = q$

### Departure from the "conventional" model in the literature

Most authors consider a propeller model with only the $\vec{k}_b$ terms in (1)-(2), i.e., with all $\lambda_i$'s and $\mu_i$'s equal to zero. Hence, the "conventional" model is the same as the revisited one but with the $\lambda_i$'s and $\mu_i$'s equal to zero in (16)–(22) and (26)– (27).

However, there is obviously a problem with such a model : indeed $\vec{a} = \dot{\vec{V}}_C - \vec{g}$ is collinear with $\vec{k}_b$, hence $a_x = a_y = 0$, which is certainly not very useful for feedback. This paradox is usually not acknowledged and the approximation $\vec{a} \approx -\vec{g}$ is used instead, i.e.,

$$(a_x, a_y, a_z) \approx (g\sin\theta, -g\sin\phi\cos\theta, -g\cos\phi\cos\theta) \tag{32}$$

The reason proposed is that $\dot{\vec{V}}_C$ is small near hovering, at least in average. This is indeed true if the aircraft is stabilized by some extraneous means (such as a human pilot), but is a questionable assumption to use from a closed loop perspective. Nevertheless, many successful flights with controllers based on this approximation have been reported. In IV-C, we suggest an explanation reconciling all of those facts in the light of the revisited quadrotor model.

The resulting "conventional" longitudinal subsystem is then

$$\dot{u} = -g\theta \tag{33}$$
$$\dot{\theta} = q \tag{34}$$
$$\dot{q} = f_4\omega_q \tag{35}$$
$$\dot{\omega}_q = \Gamma_q - f_5\omega_q \tag{36}$$

with measurements $a_x = g\theta$ and $g_y = q$, to be compared with (28)–(31) with measurements $a_x = -f_1 u$ and $g = q$

## Experimental validation

### Experimental setup

To validate the model, we recorded flight data with our home-built "Quadricopter", see figure 1. Due to limitations of our experimental setup, we could collect data to validate only the force model (28), but not the moment model (30); this is nevertheless the most important part of the model, since it accounts for the accelerometer measurements. The quadrotor was fitted with a MIDG2 "GPS-aided Inertial Navigation System"3 and a radio data link to the ground station. The MIDG2 consists of a triaxial accelerometer, a triaxial gyroscope, a triaxial magnetometer, a GPS engine and an on-board computer. The raw measurements are fused by an EKF on the onboard computer to

provide estimates of the orientation and of the velocity vector with respect to the Earth axes. The MIDG2 is an "independent" device with no knowledge of the specific system that it is fitted on; it heavily relies on the GPS engine for good dynamic estimates, without using assumption (32). All of the data can be issued at a pace of up to 20 ms. Due to the low throughput of the radio data link, only the accelerometer raw measurements $a_{xm}$, $a_{ym}$ and the MIDG2-computed quantities $\phi_m, \theta_m, \psi_m$ and $V_x, V_y, V_z$ were transmitted to the ground station, at the reduced pace of 40 ms.

We flew the quadrotor performing repeated back and forth translations at a (nearly) constant altitude and recorded one minute of flight data. Since a GPS module is used, the test was conducted outdoors, on a very calm day to respect the no-wind assumption.

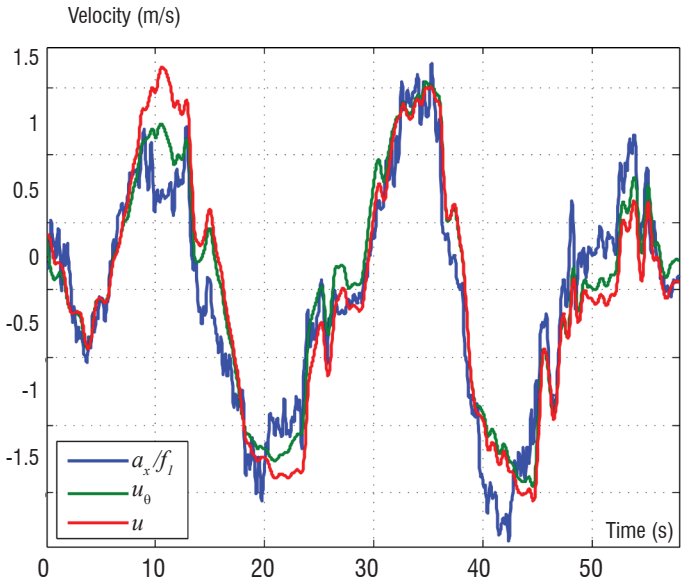


Figure 3 - Comparison between $\frac{a_x}{f_1}, u_\theta$ and $u$

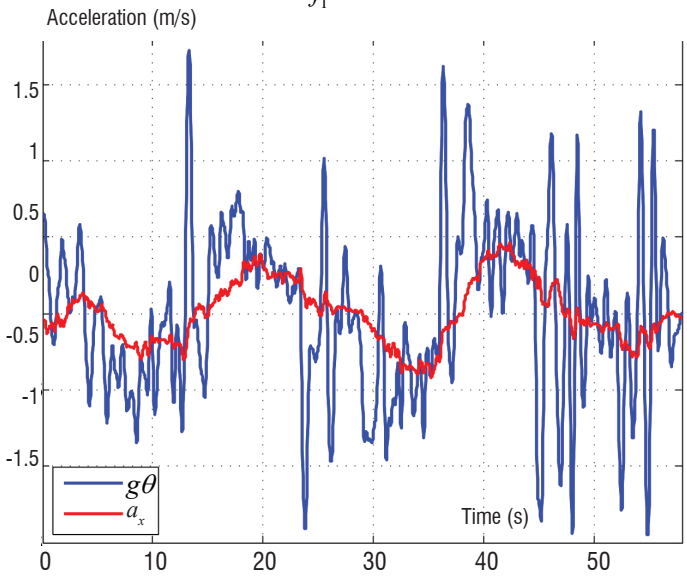


Figure 4 - Comparison between $a_x$ and $g\theta$

## Validation of the force model

Due to an imperfect mechanical design of our quadrotor, the MIDG2 case is not exactly aligned with the quadrotor frame, but rather tilted by the unknown (small) angles $\phi_0, \theta_0, \psi_0$ . The angle and acceleration data must be rotated accordingly to be expressed with respect to the quadrotor axes (the velocity data requires no correction, since it is expressed relative to the Earth axes), that is

$$(\phi, \theta, \psi) = (\phi_m - \phi_o, \theta_m - \theta_0, \psi_m - \psi_0)$$

$$\begin{pmatrix} a_x \\ a_y \\ a_z \end{pmatrix} = R^T_{\phi_0,\theta_0,\psi_0} \begin{pmatrix} a_{xm} \\ a_{ym} \\ a_{zm} \end{pmatrix}$$

Dropping higher-order terms, this yields

$$a_x \approx a_{xm} - \psi_0 a_{ym} + \theta_0 a_{zm} \approx a_{xm} - \theta_0 g$$

$$a_y \approx \psi_0 a_{xm} + a_{ym} - \theta_0 a_{zm} \approx a_{ym} - \phi_0 g$$

The velocity vector in relation to the body axes is obtained by

$$\begin{pmatrix} u \\ v \\ w \end{pmatrix} = R_{\phi,\theta,\psi} \begin{pmatrix} V_x \\ V_y \\ V_z \end{pmatrix}$$

and is considered as the "true" reference velocity to validate our modeling assumptions.

We also wanted to compute the velocities $u_\theta$ and $u_\phi$ predicted by the integration of the linearized force model (28)

$$\dot{u}_\theta = -f_1 u_\theta - g\theta$$

$$\dot{v}_\phi = -f_1 v_\phi + g_\phi$$

with initial conditions $u(0)$ $u(0)$ and $v_\phi(0) = v(0)$ .

The task was then to adjust $f_1, \phi_0, \theta_0, \psi_0$ to get a good fit between $-\frac{a_x}{f_1}, u$ and $u_\theta$ on the one hand, and between $-\frac{a_y}{f_1}, v$ $v$ and $v_\phi$ on the other hand. Since the accelerometer data are quite noisy and requires some filtering, the same filter (5th order Bessel filter with 2 Hz cutoff frequency) was applied to all of the data, in order to preserve the transfer functions among them.

With $(f_1, \phi_0, \theta_0, \psi_0) = (0.25s^{-1}, 1.2°, -2.4°, 2°)$ the agreement is good between the "true" (i.e., MIDG2-given) velocity $u$, the "accelerometer-based" velocity $-\frac{a_x}{f_1}$ and the velocity $u_\theta$ "predicted" by the model from the "true" (MIDG2-given) pitch angle, see figure 3, which reasonably validates our force model. The agreement between $v, -a_y / f_1$ and $v_\phi$ not shown for lack of space, is equally good.

To test the conventional approximation (32) we also plotted $(a_x, g\theta)$, see figure 4. Though the trend is roughly correct, the fit is much worse ; the result is similar for $(a_y, -g\phi)$.

## Other validations of the force model in the literature

Since the publication of [19] several authors have experimentally confirmed (using a motion tracking system) the proposed force model [21], [22], [23].

## Implications for control schemes

We now investigate the relevance of the revisited model in the presence of a feedback controller, with (section IV-A) and without (sections IV-B and IV-C) velocity measurements. We use the numerical values

$(f_1, f_2, f_3, f_4, f_5) = (0.25, 0.76, -9.8, 0.34, 12.74)$

$f_1$ was determined from flight tests and $f_4, f_5$ were determined from static tests on the motor-propeller subsystems. The aerodynamic coefficients $f_2, f_3$ were derived analytically ; their values are plausible but nevertheless questionable.

### Two-time-scale "full-state" feedback

We first assume that the entire state is known, or which turns out to be equivalent, that $u$ and $q$ are measured without noise so that they can be used in ideal Proportional-Derivative (PD) controllers. It is customary to design a two-time-scale control law, with a fast inner loop to control $q, \omega_q$ and a slow outer loop to control $u, \theta$.

The fast inner loop is the ideal PD controller

$$\Gamma_q = -\frac{k_p}{\varepsilon^2} q - \frac{k_d}{\varepsilon} \dot{q} + \frac{k_p}{\varepsilon^2} q_r$$

where $q_r$ is the desired pitch rate ; $k_p, k_d$ are the PD gains and $\varepsilon > 0$ is a "small" parameter. Applying this feedback to (28)-(31) yields

$$\dot{u} = -f_1 u - g\theta$$
$$\dot{\theta} = q$$
$$\varepsilon \dot{q} = f_4 \tilde{\omega}_q + \mathcal{O}(\varepsilon)$$
$$\varepsilon \dot{\tilde{\omega}}_q = -k_p q - f_4 k_d \tilde{\omega}_q + k_p q_r + \mathcal{O}(\varepsilon)$$

where $\tilde{\omega}_q = \varepsilon \omega_q$ . From standard arguments of singular perturbation theory [24], the convergence of the fast variables is up to order $\varepsilon$ ruled by the well-known coefficient $f_4$ and the PD gains ; and the behavior of the slow variables $u, \theta$ is up to order $\varepsilon$ ruled by the slow approximation

$$\dot{u} = -f_1 u - g\theta \tag{37}$$

$$\dot{\theta} = q_r \tag{38}$$

Hence, the role of the aerodynamic coefficients $f_2, f_3$ is marginal if the inner loop is fast enough.

The slow outer loop is the ideal PD controller

$$q_r = k_1 u + k_2 \dot{u} - k_1 u_r$$

where $u_r$ is the desired velocity and $k_1, k_2$ the PD gains. Applying this feedback to (37)-(38) yields

$$\dot{u} = -f_1 u - g\theta$$

$$\dot{\theta} = (k_1 - f_1 k_2) u - g k_2 \theta - k_1 u_r$$

with characteristic polynomial $s^2 + (f_1 + g k_2) s + g k_1$. A reasonable closed-loop settling time is of about 1s, which requires $g k_1 = 6^2$ and $f_1 + g k_2 = 6\sqrt{2}$. This means that $f_1 = 0.25$ is negligible with respect to the effect of the controller.

We thus see that the revisited moment equation (30) does not really matter if the gyroscope measurements are good enough for a fast loop, which is usually the case in practice; nevertheless, taking into account $f_2$ and especially $f_3$ may help to design a better inner loop. As for the force model (28), it does not really matter either, provided that a velocity measurement is available, which agrees with [5]. The importance of $f_1$ is nevertheless paramount to account for the accelerometer measurements, as will be seen in the following sections.

### Conventional interpretation of accelerometer feedback

Once the inner loop is closed, the usual slow model is

$$\dot{u} = -g\theta$$

$$\dot{\theta} = q_r$$

with measurement $a_x = g\theta$. Since the velocity $u$ is clearly not observable, the role of the outer loop is simply to control the measured angle $\theta$. In theory, the simple proportional feedback

$$q_r = k(\theta_r - \frac{a_x}{g})$$

does the trick, but in practice the accelerometer measurements are too noisy to be used directly (not only because of the intrinsic sensor noise, but also because of mechanical vibrations). Instead, an "angle estimator" is often used, based on the model $\dot{\theta} = q$ with measurements $a_x = g\theta$ and $g_y = q$. A more elaborate estimator, for example an EKF or a nonlinear observer, can also be used, see the references in the introduction; it is then based on the nonlinear kinematic equations (13)–(15) and relies on the approximation (32). Whatever the filter, the first-order approximation is essentially the linear observer

$$\dot{\hat{\theta}} = g_y + l(\frac{a_x}{g} - \hat{\theta})$$

it can also be seen as a complementary filter, since its transfer function is $\hat{\theta} = \frac{s}{s+l}\theta_q + \frac{l}{s+l}\theta_{a_x}$ where $\theta_q = \frac{q}{s}$ is the pitch angle obtained from gyro integration and $\theta_{a_x} = \frac{a_x}{g}$ is the pitch angle given by the accelero.

The outer loop is thus the controller-observer

$$q_r = k(\theta_r - \hat{\theta}) \tag{39}$$

$$\dot{\hat{\theta}} = q + l\left(\frac{a_x}{g} - \hat{\theta}\right) \tag{40}$$

Applied to the usual model and defining the observation error $e_\theta = \hat{\theta} - \theta$ it yields the closed-loop system

$$\dot{u} = -g\theta$$

$$\dot{\theta} = k(\theta_r - \theta - e_\theta)$$

$$\dot{e}_\theta = -l e_\theta$$

For $\theta_r$ constant, the last two equations have the unique steady state $(\theta, e_\theta) = (\theta_r, 0)$. The characteristic polynomial is $\Delta_0 = (s+k)(s+l)$, and the closed-loop transfer functions are

$$\theta = \frac{k}{s+k}\theta_r \tag{41}$$

$$u = \frac{-gk}{s(s+k)}\theta_r \tag{42}$$

Provided that $k, l > 0$ we have as desired $(\theta, e_\theta) \to (\theta_r, 0)$, while $u$ grows linearly unbounded. For robustness, a good tuning of (39)-(40) requires that the controller and observer act in distinct time

scales (Loop Transfer Recovery), i.e., $l >> k$ or $k>>l$. We consider in the sequel a "slow" observer, which is representative of commercial "angle sensors" such as the 3DM-GX, and a "fast" controller ; for a settling time of about $1s$, we choose for example $k = 1/0.3$ and $l = 1/12$

We tested this control scheme experimentally, with a rather satisfying result : the angle $\theta$ reaches the desired $\theta_r$, though the dynamics are somewhat more sluggish than expected. The usual analysis could thus be considered as reasonably justified. Nevertheless, it does not account for the following experimental observations already visible to the naked eye :

- when pushed away from hovering, the quadrotor returns to hovering (of course at a different position)
- when flying at a constant velocity $u$ , the angle $\theta$ is not zero, but rather approximately proportional to $u$
- in response to a constant $\theta_r$, $u$ does not grow unbounded, but rather reaches a value approximately proportional to $\theta_r$.

Though these experimental facts are well-known to people in the field, they do not seem to be reported in the literature. The discrepancy is usually attributed to the neglected second order aerodynamical drag and the inevitably imperfect experimental conditions. Another more subtle discrepancy is that the observer gain $l$ must be smaller than that predicted by the theory, in order to avoid a badly damped transient (e.g., $l=1/3$ does not work well in practice).

As will be seen in the following section, these experimental facts can be explained by the revisited model.

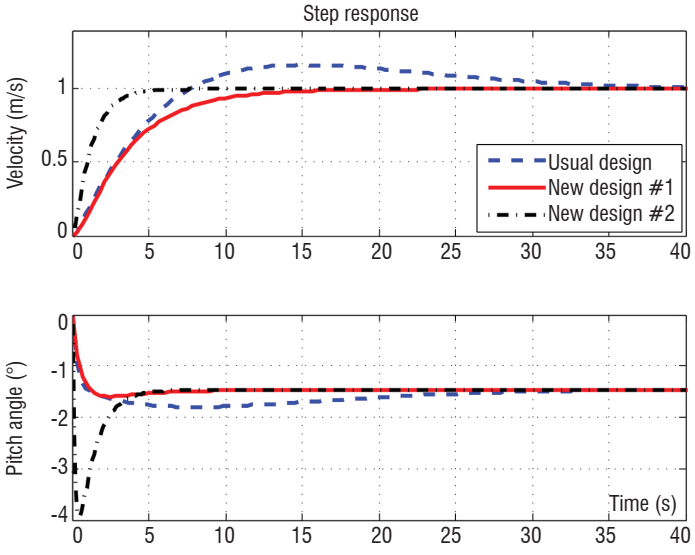


Figure 5 - Comparison between control schemes (simulation)

## Revisited interpretation of accelerometer feedback

We now apply the controller-observer (39)-(40) to the revisited longitudinal model. The closed-loop system is now

$$\dot{u} = -f_1 u - g\theta$$

$$\dot{\theta} = k(\theta_r - \theta - e_\theta)$$

$$\dot{e}_\theta = -l\left(\frac{f_1}{g}u + \theta + e_\theta\right)$$

with $e_\theta = \hat{\theta} - \theta$. For $\theta_r$ constant, the only steady state is $(u, \theta, e_\theta) = (-\frac{g}{f_1}\theta_r, \theta_r, 0)$; the characteristic polynomial is

$$\Delta = s^3 + (k + l + f_1)s^2 + f_1(k + l)s + f_1 kl$$

If $k >> l, \Delta \simeq (s + k)(s^2 + f_1 s + f_1 l)$ so that the closed-loop system is stable as soon as $k,l>0$. Hence $\theta \to \theta_r$ as desired, and $e_\theta \to 0$ as expected from the observer ; $u$ now tends to the finite value $-\frac{g}{f_1}\theta_r$ which is more consistent with experimental tests. If moreover $l << f_1$, $\Delta \approx (s + f_1)(s + k)(s + l) = (s + f_1)\Delta_0$

As a consequence, the closed-loop transfer functions are

$$\theta = \frac{k(s + f_1)(s + l)}{\Delta}\theta_r \approx \frac{k}{s + k}\theta_r$$

$$u = \frac{-gk(s + l)}{\Delta}\theta_r \qquad \approx \frac{-gk}{(s + f_1)(s + k)}\theta_r$$

to be compared with (41)-(42) : the angle dynamics is nearly the same as that given by the usual interpretation, while the velocity dynamics is dominated by the rotor drag time constant $1/f_1$. Defining the reference velocity $u_r = -g/f_1\theta_r$ we see that the usual control scheme, designed as an angle controller, is in fact a velocity controller!

The behavior experienced in practice is qualitatively and quantitatively well predicted by the revisited model, see figure 5 ("usual design"), the time response to a $-1.5°$ step in $\theta_r$ (i.e. a $1\ m/s$ step in $u_r$).

From this analysis, we see that the importance of the coefficient $f_1$ is paramount : the usual scheme works reasonably well only because $f_1$ is positive and not too small.

## A better control law

The performance of the usual control scheme is limited by the rotor drag time constant $1/f_1$ . Better performance can be achieved by considering a controller-observer based on the revisited model,

$$q_r = -k_1\hat{u} - k_2\hat{\theta} + \left(k_1 - \frac{f_1 k_2}{g}\right)u_r$$

$$\dot{\hat{u}} = -f_1\hat{u} - g\hat{\theta} + l_1(a_x + f_1\hat{u})$$

$$\dot{\hat{\theta}} = g_y + l_2(a_x + f_1\hat{u})$$

where $u_r$ is the velocity reference, $k_1, k_2$ are the controller gains and $l_1, l_2$ are the observer gains. Figure 5 shows simulation results for the same scenario as before (1 m/s reference step in velocity). Two different tunings were used: in the first case ("New Design #1") the controller is tuned for a settling time of about 12 s and the observer is tuned for about 48 s, so that the angle and velocity have initial transients similar to the tuning used previously for the usual design

(and with a similar control effort); in the second case ("New Design #2") the controller is made four times faster.

Both designs were successfully implemented, resulting in a quadrotor that is much easier to fly than with the usual scheme. In practice, it was difficult to accelerate the time responses much further, probably mainly due to accelerometer noise.

## Conclusion

We have proposed and experimentally verified a revisited model of the quadrotor. It is different, even at first-order, from the model usually considered in the literature. It gives a different interpretation of accelerometer measurements and explains why control schemes based on the conventional model nevertheless behave reasonably well ■

### Acronyms

EKF (Extended Kalman Filter)
GPS (Global positioning system)
MEMS (Micro Electro Mechanical Systems)
UAV (Unmannned Aerial Vehicle)

### References


[1] D. MELLINGER, N. MICHAEL and V. KUMAR - *Trajectory Generation and Control for Precise Aggressive Maneuvers with Quadrotors*. International Journal of Robotics Research, vol. 31, n°. 5, pp. 664–674, 2012.
[2] N. GUENARD, T. HAMEL and V. MOREAU - *Dynamic Modeling and Intuitive Control Strategy for an "X4-Flyer*. Int. Conf. on Control and Automation, 2005, pp. 141–146.
[3] F. KENDOUL, D. LARA, I. FANTONI-COICHOT and R. LOZANO - *Real-Time Nonlinear Embedded Control for an Autonomous Quadrotor Helicopter*. Journal of Guidance, Control, and Dynamics, vol. 30, n°. 4, pp. 1049– 1061, 2007.
[4] S. SALAZAR-CRUZ, J. ESCAREÑO, D. LARA and R. LOZANO - *Embedded Control System for a Four-Rotor UAV*. International Journal of Adaptive Control and Signal Processing, vol. 21, n°. 2-3, pp. 189–204, 2007.
[5] G. HOFFMANN, H. HUANG, S. WASLANDER and C. TOMLIN - *Quadrotor Helicopter Flight Dynamics and Control : Theory and Experiment*. In Collection of Technical Papers - AIAA Guidance, Navigation, and Control Conference 2007, vol. 2, 2007, pp. 1670–1689.
[6] S. GRZONKA, G. GRISETTI and W. BURGARD - *Towards a Navigation System for Autonomous Indoor Flying*. IEEE Int. Conf. on Robotics and Automation, 2009, pp. 2878–2883.
[7] S. BOUABDALLAH and R. SIEGWART - *Full Control of a Quadrotor.* IEEE/RSJ Int. Conf. on Intelligent Robots and Systems, 2007, pp. 153– 158.
[8] N. GUENARD, T. HAMEL and R. MAHONY - *A Practical Visual Servo Control for an Unmanned Aerial Vehicle.* IEEE Transactions on Robotics, vol. 24, n°. 2, pp. 331–340, 2008.
[9] F. KENDOUL, I. FANTONI and K. NONAMI - *Optic Flow-Based Vision System for Autonomous 3D Localization and Control of Small Aerial Vehicles.* Robotics and Autonomous Systems, vol. 57, n°. 6-7, pp. 591–602, 2009.
[10] M. ACHTELIK, A. BACHRACH, R. HE, S. PRENTICE and N. ROY - *Stereo Vision and Laser Odometry for Autonomous Helicopters in GPS-Denied Indoor Environments.* Proc. SPIE, vol. 7332, n°. 1, 2009, pp. 733 219–10.
[11] A. BACHRACH, S. PRENTICE, R. HE and N. ROY - *Range-Robust Autonomous Navigation in GPS-Denied Environments*. Journal of Field Robotics, vol. 28, n°. 5, pp. 644–666, 2011, cited By (since 1996)19.
[12] P. POUNDS, R. MAHONY and P. CORKE - *Modelling and Control of a Quad-Rotor Robot. Australasian Conf*. on Robotics and Automation, 2006.
[13] L. DERAFA, T. MADANI and A. BENALLEGUE - *Dynamic Modelling and Experimental Identification of Four Rotors Helicopter Parameters.* IEEE Int. Conf. on Industrial Technology, 2006, pp. 1834–1839.
[14] T. MADANI and A. BENALLEGUE - *Backstepping Control with Exact 2- Sliding Mode Estimation for a Quadrotor Unmanned Aerial Vehicle.* IEEE/RSJ Int. Conf. on Intelligent Robots and Systems, 2007, pp. 141–146.
[15] P.-J. BRISTEAU, P. MARTIN, E. SALAÜN and N. PETIT - *The Role of Propeller Aerodynamics in the Model of a Quadrotor UAV*. European Control Conf., 2009, pp. 683–688.
[16] P. MARTIN and E. SALAÜN - *Design and Implementation of a Low-Cost Observer-Based Attitude and Heading Reference System*. Control Engineering Practice, vol. 18, no. 7, pp. 712 – 722, 2010.
[17] P. MARTIN and E. SALAÜN - *An Invariant Observer for Earth-Velocity Aided Attitude Heading Reference Systems.* IFAC World Congress, 2008, paper identifier 10.3182/20080706-5-KR-1001.3577.
[18] P. D. GROVES - *Principles of GNSS, Inertial, and Multisensor Integrated Navigation Systems*. Artech House, 2008.
[19] P. MARTIN and E. SALAÜN - *The True Role of Accelerometer Feedback in Quadrotor Control.* IEEE International Conference on Robotics and Automation, 2010, pp. 1623–1629.
[20] W. JOHNSON - *Helicopter Theory*. Princeton University Press, 1980.
[21] P.-J. BRISTEAU, F. CALLOU, D. VISSIÈRE and N. PETIT - *The Navigation and Control Technology Inside the ar.Drone micro UAV*. IFAC World Congress, 2011, pp. 1477–1484, paper identifier 10.3182/20080706- 5-KR-1001.3577.
[22] J. MACDONALD, R. LEISHMAN, R. BEARD and T. MCLAIN - *Analysis of an Improved Imu-Based Observer for Multirotor Helicopters*. Journal of Intelligent & Robotic Systems, pp. 1–13, 2013.
[23] D. ABEYWARDENA, S. KODAGODA, G. DISSANAYAKE and R. MUNASINGHE - *Improved State Estimation in Quadrotor MAVs: A Novel Drift-Free Velocity Estimator*. IEEE Robotics Automation Magazine, vol. 20, n°. 4, pp. 32–39, 2013.
[24] P. KOKOTOVIC, H. K. KHALIL and J. O'REILLY - *Singular Perturbation Methods in Control : Analysis and Design*. SIAM, 1999.

## AUTHOR

**Philippe Martin** received the PhD degree in Mathematics and Control from the Ecole des Mines de Paris in 1992, where he is currently a Senior Researcher. In 1993-1994 he visited the Center for Control Engineering and Computation of the University of California at Santa Barbara and the Department of Mathematics of the University of North Carolina at Chapel Hill. Since 2000 he has also been a part-time Professor at Ecole Centrale Paris. His interests include theoretical aspects of nonlinear control and their applications to industrial control problems.